

Review

Diamond-Like Carbon (DLC) Coatings: Classification, Properties, and Applications

Dipen Kumar Rajak ^{1,*}, Ashwini Kumar ², Ajit Behera ³ and Pradeep L. Menezes ^{4,*}

¹ Department of Mechanical Engineering, Sandip Institute of Technology & Research Centre, Nashik 422213, India

² Department of Mechanical Engineering, Faculty of Engineering & Technology, SGT University, Gurugram, Delhi-NCR 122006, India; aknitjsr08@gmail.com

³ Department of Metallurgical and Materials Engineering, National Institute of Technology, Rourkela 769008, India; ajit.behera88@gmail.com

⁴ Department of Mechanical Engineering, University of Nevada, Reno, NV 89557, USA

* Correspondence: author email: dipen.pukar@gmail.com (D.K.R.); pmenezes@unr.edu (P.L.M.)

Abstract: DLC coatings have attracted an enormous amount of interest for science and engineering applications. DLC occurs in several different kinds of amorphous carbon materials. Owing to the extensive diversity in their properties, DLC coatings find applications in mechanical, civil, aerospace, automobile, biomedical, marine, and several other manufacturing industries. The coating life of DLC is predominately influenced by its constituent elements and manufacturing techniques. Numerous researchers have performed multiple experiments to achieve a robust understanding of DLC coatings and their inherent capabilities to enhance the life of components. In this review, a wide range of DLC coatings and their classification, properties, and applications are presented. Their remarkable performance in various applications has made DLC coatings a promising alternative over traditional solitary-coating approaches.

Keywords: DLC.; coating; low friction; DLC applications; DLC properties; DLC classifications

Citation: Rajak, D.K.; Kumar, A.; Ajit, B.; Menezes, P.L. Diamond-Like Carbon (DLC) Coatings: Classifications, Properties, and Applications. *Appl. Sci.* **2021**, *11*, 4445. <https://doi.org/10.3390/app11104445>

Academic Editors: Witold Kaczorowski, Damian Batory and Alberto Milani

Received: 25 March 2021

Accepted: 10 May 2021

Published: 13 May 2021

Publisher's Note: MDPI stays neutral with regard to jurisdictional claims in published maps and institutional affiliations.



Copyright: © 2021 by the authors. Licensee MDPI, Basel, Switzerland. This article is an open access article distributed under the terms and conditions of the Creative Commons Attribution (CC BY) license (<http://creativecommons.org/licenses/by/4.0/>).

1. Introduction

DLC is a group of indistinct carbon (C) materials with the unique property of a diamond. Several techniques have been used for the coating process of different material composites, which make them more superior and multi-purpose applications, including biomedical and marine engineering [1]. Moreover, DLC has a large scale of sp^3 hybridized C molecules as a diamond, and discloses their seven distinctive forms.

DLC coatings are made through the mixing of poly-type, as a different form in nano-scale of structures that simultaneously are formless and adaptable, but are then only sp^3 reinforced like a diamond. The hardest and most grounded is such a blend, referred to as tetrahedral amorphous carbon (ta-C). For instance, a covering of just 2 μm of ta-C expands the obstruction of stainless steel against rough wear, changing its lifespan from a week to 85 years. Such ta-C can be viewed as the “unadulterated” type of DLC, as it comprises only sp^3 -reinforced C ions. Fillers, for example, hydrogen (H), graphitic sp^2 C, and metals, are utilized in the other six structures to decrease manufacturing costs [2,3]. In October 2011, Science Daily announced that researchers at Stanford University had made a super-hard shapeless diamond under states of ultrahigh-pressure conditions that came up short on the translucent structure of diamond [4]. Normally, diamond is quite often found in a glass-like structure with a cubic direction of sp^3 -reinforced C ions.

The inner energy of the cubic poly-type is smaller than the hexagonal structure and growth rates from liquid material in both (i.e., normal and heavy) diamond manufacturing techniques. Meanwhile, they are moderate enough that cross-section structures have

the opportunity to fill the least energy (cubic) structure and are feasible for sp^3 bonding of C ions, whereas DLC is normally synthesized, utilizing rapid cooling on high-energy preliminary C on cool surfaces. In such a case, cubic and hexagonal lattices are combined with several layers, a very short period time elapses for either lattice to produce over another, and prior molecules become frozen. A few methods introducing DLC depend on the lower density of sp^2 and then on sp^3 C. So, the synergic effects of pressure, impact, and catalysis at the microscopic level constrain sp^2 particles closer into sp^3 bonds. Typically, this is achieved by introducing a group of new sp^3 C along with the pressure in the depth of the coating, leaving no space for sp^2 detachments, or the new group is covered by the appearance of a new C-bond for the upcoming pattern of effects. They occur separately at many spots marked on films or coatings. In addition, DLC reveals unique types of undefined C materials. Herein, it has been observed that DLC coatings were discovered for numerous applications in several engineering works, including biomedical, marine, and other assembling ventures. The covering life of DLC is based on its constituent components and manufacturing methods. Thus, the practical properties of different constituents accessible worldwide, their characterizations, and properties to be concentrated, have to distinguish the enhanced material properties for the ideal application. An outline of a different scope of DLC coatings, characterization, properties, and applications is introduced here.

Historical Background of DLC

Indistinct DLC coatings reveal exceptionally smooth surfaces, resistance to wear, and low-friction behavior. Nowadays, DLC films are utilized globally in a wide range to improve apparatuses and segment quality, particularly for automobile applications [5–9], with greater than 100 million covered parts for every year and a market volume of approximately EUR 100 million.

In 1953, Schmellenmeier introduced C-films using acetylene gas instead of tungsten-cobalt alloy [10]. The significant outcome of the experiment was to achieve a thin sheet of tungsten carbide (WC) produced by glow discharge in the presence of hydrocarbons at low temperatures. In continuation of the same work, it was observed that black hard formless layers were set up at the cathode pole as long as the flow rate of current was low. However, thick (μm) hard films were recognized as diamonds after performing X-ray diffraction (XRD) [11]. In 1951, König and Helwig [12] investigated direct current (DC) through the glow-discharge process in a benzene (C_6H_6) atmosphere. However, they analyzed only the film grown on the discharged anode, and the films had a yellow color and comparatively low-density. Hereafter, Heisen [13,14] investigated that more films with high density were deposited on the cathode compared to the anode, which showed that positive particles had larger cross-sections than negatively charged particles. Heisen [13] found that the films' growth rate significantly depended on the substrate geometries, while those protecting the substrate were charged under ion-bombardment then stopped the film growth. The term DLC was initially introduced by Aisenberg and Chabot [15] in 1971, the layers were formed at ambient temperature, making use of ion beam deposition technique, which involves C, argon (Ar) particles, and a graphite electrode. After examination, it was determined that films showed optical transparency, resistance to wear, and electrical and chemical flow. The film structure was described as partly crystalline, having lattice parameters the same as diamond. In 1971, Aisenberg et al. reported improvement of cutting performance of paper-cutting blades by employing DLC coatings. When the blades were tested for wear, they found a decrease in frictional coefficient [16]. Spencer et al. [17] investigated DLC coating performance like Aisenberg and Chabot [15]. Whitnell and Williamson [18] organized hard and protecting coatings of up to 4 μm thickness on various metal surfaces utilizing the ion beam deposition method of Schmellenmeier and Heisen, but used a gas combination of ethylene (C_2H_4) along with 5% Ar. The protective layer required to hold a positive charge attaining maximum thickness should be normal. Holland [19] clarified this, expecting that secondary electrons produced at the boundary of the domed aperture compensate for the positive charge. Later, the result was confirmed

for a DC-based particle plating a-C: H measure on protecting glass substrates [20]. Throughout the tenure, new techniques like responsive faltering and cathodic circular segment measures as changes of diamond-like indistinct C-based films were made. Now, a maximum utilization, particularly in the automobile, has been set up, and, for example, for diesel infusion system, DLC coatings are essential.

2. Classification of DLC Coatings

DLC is a type of thin-film material of amorphous carbon (a-C) or hydrogenated amorphous carbon (a-C: H), which has a high binding rate of the metastable sp^3 C bond. These particles provide an ascent for the sp^3 bond, which is in stark contrast to the sp^2 bond unless balanced by the C-H bond. It has been suggested that cyclic particles are different from plasma polymerization. In this reaction, with the development of subatomic H_2 , the accumulation of C-H groups will form C sp^3 bonds. The DLC can be linked with different compositions (such as Si and F). This section discusses unalloyed materials first, rather than specifying alloyed materials. Specifically, it has four bases: (1) processing, (2) structure, (3) properties, and (4) performance, and improves the bond between them—each edge of the tetrahedron is connected at the edge to each other corner [21].

However, academicians and industrial researchers have turned their attention toward the development of DLC coatings due to excellent optimization among tribological, mechanical, and chemical properties. DLC coatings are deployed in automotive engines because of superior friction behavior, increased life cycle, and compatibility with chemicals because of their inert nature. However, such kinds of properties will be influenced by mixing nonmetals and metals (see Figure 1).

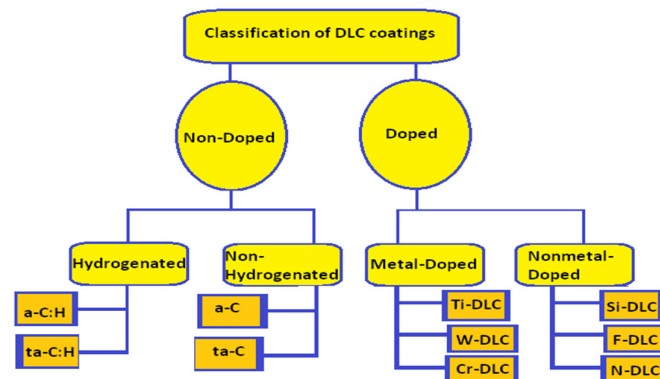


Figure 1. The general classification of DLC coatings.

In this classification section, the sp^3 ratio, H content, and other properties of several types of C-films were studied to categorize the amorphous C-films, including DLC. The results demonstrated that amorphous C exists in a wide range in the ternary diagrams of sp^2 , sp^3 , and H. Subsequently, amorphous C was categorized in four groups of the DLC region and one group of the PLC region. Herein, the percentage contribution factors of categorized groups were observed as ta-C content $>50\%$ of sp^3 ratio and $<5\%$ of H. At the same time, a-C content was $<50\%$ of sp^3 ratio and $<5\%$ of H. As they categorized four DLC regions, it was more reasonable to classify these DLC groups as polymer-like C-films rather than DLC films. The maximum level of sp^3 ratio was expected to suppress film corrosion, due to mellite reactions for corrosion resistance; therefore, this was almost distinct from the sp^3 ratio. Typically, it has been introduced to internationally standardize C-films, including DLC, without disclosing data, and reports have been published as ISO20523:2017 [22]. The major findings of this study are expected to serve as a basis for deriving the sp^3 ratio and H content at high precision using XPS and glow-discharge optical emission spectroscopy. DLC films can be further classified as a biocompatible material [23] in a refraction index plane and extinction coefficient [24], which can help in large-

scale development and industrial applications. However, as per ISO 20523:2017 disclosed of the standard specifies classification, and designations, and predominant constituent on DLC films. Amorphous C-based films are also known as DLC, as well as graphite, polymer-like films, and CVD diamond films. This applies to mass-production on an industrial scale, which is appropriate for the C-based films. However, it does not apply to the entire coating, and it can be made up of a main functional layer and additional layers on the top and bottom. Over the development of its thickness, a material's property may be changed. These kinds of layers are known as gradient layers. C-based films can include other elements like H, metal, and other elements. Metal carbide can be used as a metal constituent with supplementary elements, and are only covered if C is the predominant constituent part. However, a detailed informative fact was found regarding the DLC films classification based on the experimental results, and their characteristics and applications are explained in different subsections.

2.1. Stage Diagram

1. The types of DLC on the ternary graph are shown in Figure 2, which also shows the division of the targets in the combination; i.e., C sp^3 , C sp^2 , or H [1], according to Jacob and Moller's recommended graph [25]. The outline of the stage consists of three main areas: (i) without H a-C along with the left pivot, (ii) sp^2 a-C is commonly lustrous C or a-C produced by dissipation, and (iii) cutting-edge variations of faltering, including uneven magnetron faltering, can make DLCs with an enormous sp^3 substance. At considerably maximum sp^3 content, there is an explicit sort of a-C assigned as tetrahedral shapeless C. This is produced using plasma particles or radiation with high particle splitting and almost no characteristic particle energy [26–29].

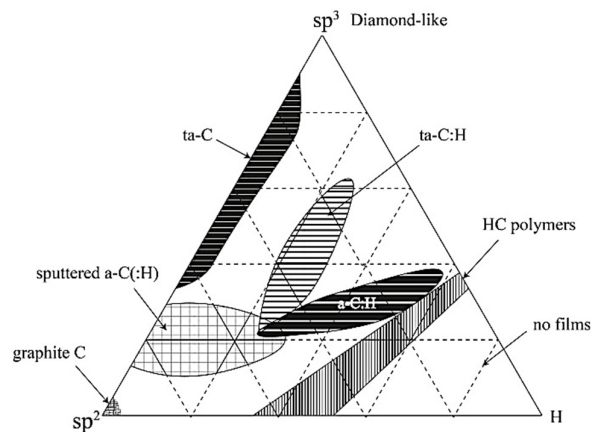


Figure 2. Ternary phase diagram of the C, H system [1].

The second position of the stage outline is in the lower right corner of the figure, where the H content is so high that the material cannot form a fully connected network, and can only form gas molecules [25]. In the center, the area in the material is a-C: H, which is usually produced by the deposition of plasma-enhanced chemical vapors (PECVD) of hydrogen atoms and C, or by the susceptible interference of graphite in air, or from the precursors of hydro C gases [30–35]. A common PECVD or staggering cycle produces a-C: H, which is located in the area referred to as a-C: H. It can go from the material by including 20 to 25% of H content up to exceptionally high, with H substance of ~60% of the total number of atoms. With the improvement of PECVD, it is conceivable to produce high-density plasma. These methods produce thicker a-C: Hs, which we call tetrahedral, hydrogenated invisible C, or ta-C: H [36,37]. High-density plasma is achieved by working at a lower pressure than typical PECVD and using a magnetic field to generate longer electron path lengths, thus promoting high plasma ionization.

In addition, since the last decade, researchers have described and revealed the development of high-level accuracy of metal-free C electrocatalysts for oxygen reduction reac-

tion (ORR), and this is one of the promising methods for the exploitation and use of renewable and clean energy; however, there still are major challenges to resolve. Meanwhile, the facile synthesis approach is arranged in such a way for three-dimensional (3D) N-doped C with a selected sp^3/sp^2 interface, which is derived from ionic liquids through shift transformation [38]. However, density functional theory reveals improved performance of ORR, and it can be ascribed to the existence of N dopants at the sp^3/sp^2 C interface [39–45].

Another investigation of DLC coatings was conducted on stainless steel (SS) employing a plasma-based particle-deposition methodology along with two different parameters [46]. Herein, specimens were characterized by several techniques, such as exploitation high-resolution elastic recoil analysis, micro scale X-ray negatron spectrometry, and nano-indentation testing to work out the chemical element content, sp^2/sp^3 magnitude relation, and mechanical properties of the coating [47,48].

2.2. Structural Arrangement

Strong C is broadly classified; i.e., ordered (diamond, nanotubes, and graphite) and disordered DLC structures. The structure of formless C comprises sp^2 - and sp^3 -hybridized C. The sp^3 -rich material has 3D organizations with completely covalent bonding. In this way, it is precisely hard and possesses moderately higher density. A density value of more than 3 g/cm^3 is described as a density near the density of diamond [49]. Then again, the sp^2 -rich material has 2D organizations with a covalent bond, a weak bond starting from intermolecular powers. In this way, this structure is precisely delicate and has a moderately low density. This material is indistinct C (a-C), which is infrequently perceived as DLC in a wide range [50]. Hydrogenated C films are additionally utilized for engineering applications.

2.3. Processing

The vapor deposition method is one of the well-known procedures applied to blend indistinct C. Vaporization methods are essentially isolated into two ways: (1) PVD and (2) CVD. As non-ionized particles are added to the film development to increase the voltage to the substrate and do not cause any changes in the structure of C: H, it is regularly added to the plasma gas for forming a-C: H films. The C bond, with around 30% ionized C particles, flows toward the substrate [51]. It additionally consists of a large number of small C particles.

In the CVD cycle, hydro C gases, for example, acetylene and methane are deteriorated synthetically and dense into the C or hydrogenated C films on the substrate. For deterioration, plasma response measures are presented, in which the dehydrogenation of the hydro C particles continues to diminish the disintegrated stress. High-plasma-density PECVD sources are proposed to create sp^3 -rich films; these sources incorporate electron cyclotron reverberation (ECR) [52], the plasma bar source (PBS) [53], and electron cyclotron wave reverberation (ECWR). These methods are completed under generally low weights [54]. In this way, the ionization capacity of gas atoms by electron sway and speeding up the level of the ionic species around the substrate is high.

2.4. Properties

2.4.1. Film Density

DLC films can be isolated into four classes, depending on film density properties: ta-C, ta-C: H, a-C, and a-C: H. The sp^3 -rich material ta-C regularly shows a high density of 3.2 g/cm^3 . For example, ta-C films were saved by FCVA (filtered cathode vacuum arc) at various substrate negative biases. Generally, a 2.71 g/cm^3 density was considered for predisposition voltage of 0 V to achieve a high density (3.42 g/cm^3) at a predisposition voltage of 80 V [55]. As the strength of the applied S-twist (two-fold curve) filter was expanded,

the plasma was engaged and limited more strongly, and a slight increment in atomic current density was identified. The materials required to produce these films were acquired from high-plasma-density PECVD sources; for example, PBS (plasma beam source) and ECWR (electron cyclotron wave reverberation) [56,57]. The energy and transition of the particles moving at the developing film surface were shifted by providing an outside voltage to the substrate [58–60].

2.4.2. sp^3 —Density Curvature

There are two types of densities with sp^3 content. First, hydrogen-free a-carbon changes linearly [61], which is predicted according to Vegard's law of alloys. The second is for a-C: H. It is ta-C: H, which can be formed from a high-density plasma source and the density, is improved with the sp^3 content. Usually, the density expands at the most extreme point, at which time the H content increases rapidly, and the huge atomic size of the C-H group translates into the highest density and decreases with a high sp^3 value. It was found that for the most part, for a-C, the FWHM amplitude of the G peak corresponded to the density. Furthermore, it was found that the dispersion of the peak wave-numbers G (dispersion G) with different excitation energies corresponded to the content of sp^3 [62–64].

2.4.3. Refractive Index

Generally, ta-C films exhibit a high refractive index, sometimes higher than diamond (2.419). In a-C films carrying a refractive index range of 1.6 to 2.6, it has been seen to be less than that of ta-c films. Even though the tests showing a refractive index above 2.0 demonstrated a moderately high extinction coefficient of over 0.1, the samples with refractive records less than 2.0 showed a moderately low extinction coefficient than 0.1 [65].

2.4.4. Growth Rates in PECVD

The precursor molecule for a-C: H development is, for the most part, picked as to the film growth rate. The growth rate is discovered to be firmly connected to the ionization capability of the atom [30]. Unsaturated atoms with low ionization possibilities; for example, acetylene, return a large number of high development rates compared to methane [65]. Acetylene is likewise preferred by several researchers, since it has the most reduced H content (alongside benzene) of the standard precursor molecule, and hence the H substance of the subsequent a-C: H film likewise will, in general, be lower [66]. As modulus of elasticity is identified with the part of C-C bonding, it makes the H content inclined to drop to increase the modulus, and accordingly the hardness, for a given sp^3 content. Subsequently, one should keep a high atomic energy of state 500 eV for each C to decrease pressure. Particle energy for each C ion demands 500 eV for methane, but 1000 eV for acetylene. An irregular mix stores a-C: H from methane at high atomic energy (600–1200 eV) [67–72].

In this way, the atomic energy is well over the ideal estimation of 100 eV compared to the highest sp^3 content. Hence, the C-bonding is partly graphitic. Yet, the high ion energy also leads to the implantation of a large part of the H atoms of the incident methane, with the goal that the film has an uncommonly higher H content for a-C: H films of sp^2 content [73,74].

2.4.5. Stress

Thick films produce intrinsic compressive stress that causes delamination of the film [1]. There are many ways to minimize this effect; for example, the use of an adhesive layer of Si, a graded adhesive layer, or multilayer or metal alloy. In this case, the average state of the particles of the film deposition is 100 eV. However, it is also subject to short pulses (~10 μ s), which have a much higher bias voltage, greater than 1000 eV. Energy particles cause stress relaxation [75,76]. The high-energy particles allow for some degree of atomic

relaxation, thus reducing stress. A limited number of sp^3 sites will be converted to sp^2 , which is enough to keep the diamond-shaped attribute. At the basic level, this cycle will act on both ta-C and a-C: H.

2.4.6. Alloyed DLCs

Novel properties of DLC are a promising way to meet the requirements for several applications, and normally they can be enhanced by alloying with other elements [77–82]. An investigation of the impact of alloying with different transition metals; (for example, Ti, Cr, and Al), was conducted. Al, in particular, was found to reduce the stress and thereby permit the growth of thicker films. These can be referred to as a-C: Me or a-C: H: Me, separately. Alloying with transition metals is additionally used to expand the mechanical strength of the films. DLC is a rather brittle ceramic, and alloying with carbide-forming metals makes it harder as a result of the development of nano-sized carbide inclusions. Furthermore, the expansion of Si to a-C: H resulted in low stress and reduced friction coefficient in humid conditions [81]. In addition, after mixing of fluorine (F), the surface energy was found to be significantly low. However, it may vary if Si, nitrogen (N), and boron (B) are added [79]. The addition of N in films has been pointed out because of the hypothetical compound, i.e., C_3N_4 , where C is sp^3 and N is sp^2 bonded [80].

3. Characterizations/Properties of DLC Coatings

3.1. DLC Substrate Compatibility

The main challenge for substrate compatibility with DLC and DLC coatings is the way of showing good adhesion. Table 1 illustrates the substrates that were used in the PECVD reactor for DLC treatment. In some cases, the DLC cannot adhere directly to the substrate (treated stainless steel). At the same time, the DLC coatings were completed using intermediate layer materials to improve the adhesion properties.

Table 1. List of DLC-compatible substrates

Kevlar	304 Stainless steel
Polyethylene PolyCate (Lexan)	440 Stainless steel
Poly (Styrenec Arylate)	Iron
Silicon (Si)	Tantalum
	Aluminum (Al)

3.2. Tribological Properties of DLC Coatings

Numerous investigations have been carried out in the field of tribology on DLC coatings since the last decade, due to its low friction coefficient and low wear resistance. One of the foremost studies published recently regarded the impact of plasma pretreatment on the wear behavior of DLC coatings on PDMS (poly-dimethyl-siloxane) substrates [83]. A technology-supported low-pressure plasma and dielectric barrier discharge (DBD) plasma was used for the very first modification procedure. The essential properties of the DLC coatings delivered on unmodified substrates were contrasted with those of the coatings influenced to plasma pretreatment. The tests exhibited a cross-linking of the polymer substrate during plasma pretreatment.

With 0.7%, 5.8%, and 23.3% Ti in DLC, coatings were applied via pulsed cathode arc deposition and magnetron sputtering on AISI 316L chrome steel substrates [84]. The variable value of Ti content was managed by setting the Ti target current at 3, 5, and 7 A. The tribological properties of Ti-doped DLC (Ti-DLC) coatings were studied using X-ray photoelectron spectroscopy, Raman spectroscopy, nano-indentation, and a ball-on-disc tribometer. The main output of this investigation regarded TiC, which formed when Ti content within the coating was above 5.8%. Ti-DLC with 0.7% Ti had the very best $\frac{H}{E}$ and $\frac{H^3}{E^2}$ ratios, and exhibited optimal tribological properties under lubrication.

In another study, soft DLC films were deposited on Si (100), iron, and chrome steel substrates with a Cr adhesive interlayer using PVD magnetron sputtering technology [85]. The major output was to connect the coating chemical and mechanical behaviors to the various deposition parameters, such as discharge power and substrate-target distance. Stronger sp^3 dependence was found on the discharge power for DLC deposited closer to the target. These tribological results were not dependent on the chosen substrate-target distance, but rather on the hardness of the substrate.

3.3. Chemical Resistance of DLC Coatings

The chemical inertness of diamond makes it attractive as a protective coating against chemical formations [86]. In this study, 2" diameter discs of 6061-T6 and 5053 Al, 1/4" thick, were metallographically polished to a 0.5 μm finish by utilizing a silica slurry and cleaned with isopropyl alcohol. After the deposition of DLC layers, the samples were tested for analyzing chemical attacks or formation on the substrate surface by using acid drops (Figure 3). The principal tests were produced by applying one layer of 1 μm to 2 μm thickness of DLC deposited on the Al substrates [87]. Further investigation was carried out for enhancing the substrate surface and deploying the SEM test examination to identify the stress cracking on the substrate surface. Al- 6061-T6 contains insolvable $(\text{FeCr})_3\text{SiAl}_{12}$ incorporations and excess Mg_2Si particles that are harder than the matrix.

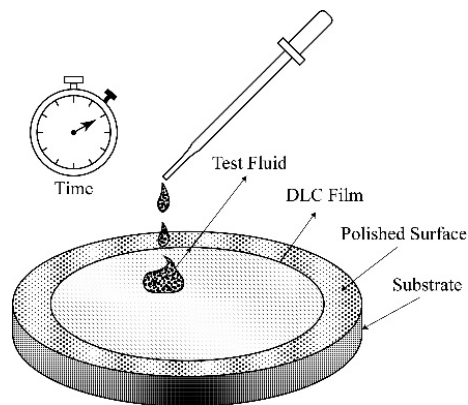


Figure 3. Diagram representing the chemical test procedure [87].

Different effects were pursued to eliminate imperfections in the DLC coatings; including the utilization of thick coatings ($\leq 2 \mu\text{m}$), different layered coatings, and silicon between interlayers. None of the coatings was completely free from the inclusion of undesirable particles. The thicker coating was moderately resistant to chemical formation compared to thinner coatings; since they expanded the ideal opportunity for acid permeation through the layer [87] (see Figure 3). For instance, with the thinner coatings, the response between the Al substrate and the acid was immediate. Utilizing various layered coatings (comprising both thin and thick layers, 0.5 μm and 1.5 μm , respectively), the protection from chemical reaction was expanded up to 20 min. At the same time, coatings with a Si layer between the DLC and Al substrate gave the best protection from permeation, delaying chemical reaction with the substrate up to 60 min. Moreover, while considering the permeation time, the effect of time on the permeation process was not completely removed by using the Si interlayer due to the inclusion particles of coating defects.

3.4. Thermal Stress: DLC Films

Stress is a significant inherent parameter of DLC deposition, as stress leads to poor adhesion. Moreover, stress is a mechanical property that can be readily measured. As in bulk materials, the crack at the interference is resolved in large part by mechanical properties.

The thermal stress at interference can be readily assumed [88–90]. Thermal stress is a big problem for DLC and diamond films due to the small coefficient of thermal expansion of diamond (see Table 2). However, if diamond films are deposited on a substrate at elevated temperature, after they cool at room temperature, the substrate will bond better than diamond over-layers. Later, the diamond film is bonded to the substrate, and the interface area will change to match that of the substrate's orientation, resulting in the development of compressive stress on films.

Table 2. Mechanical and thermal properties of various materials.

Materials	Linear Coefficient of Thermal Expansion (at 20 °C) $\times 10^{-6} \text{C}^{-1}$	Modulus of Elasticity $\times 10^{11}$ (Pa)	Density (g cm^{-3})	Reference
Al	23	0.706	2.702	[91–93]
Al ₂ O ₃	5.3	4.0	3.965	[91,93,94]
Chromium	5.0	2.79	7.20	[91–93]
Cu	16.7	1.298	8.92	[91–93]
Diamond	1.0	9.1	3.51	[91,93,94]
Germanium	5.7	-----	5.35	[91–93]
Glass	4–9	0.48–0.83	-----	[91,95]
Graphite	7.8	-----	2.25	[91–93]
Fe	11.8	1.523–2.114	7.86	[91–93]
Molybdenum	5.0	3.248	10.2	[91–93]
Ni	12.8	1.995–2.192	8.9	[91–93]
Platinum	8.9	1.67	21.45	[91–93]
Si	2.5	6.6	2.33	[91,93,96]
SiC	3.7	4.8	3.217	[91,93,94]
SiO ₂	11.2	-----	2.64	[91–93]
NaCl	42.3	-----	2.165	[91–93]
Stainless Steel	15.9	2.153	-----	[91–93]
Ti	8.6	4.7	4.5	[91–93]
Tic	6.2	-----	4.93	[91–93]
Tungsten	4.5	4.11	19.35	[91–93]
Uranium	14.1	-----	19.05	[91–93]

The stress due to the thermal expansion mismatch between a substrate and over-layer can be determined utilizing Equation (1):

$$\sigma = \frac{E(\alpha_f - \alpha_s)\Delta T}{(1 - \nu)} \quad (1)$$

where σ : stress; E : modulus of elasticity; α_f and α_s : average coefficients of expansion of film and substrate, respectively; ΔT : change in temperature; and ν : Poisson's ratio. Accepting that the thermal coefficient of growth of the DLC film was equivalent to diamond and that Poisson's ratio is 0.2 [90], the pressure in a thin film was determined to be 1.4×10^8 Pa compressive stress. The range of measured stress values for a film on Si may vary between 5×10^8 and 4×10^9 Pa (see Table 3).

Table 3. Quantitative stress measurements for DLC and diamond films.

Film Stress (Pa) (C) = compressive (T) = tensile	Film composition	Deposition process	Reference
5. To 7×10^9 (C)	DLC on glass	Glow discharge	[97]
5×10^8 (C)	DLC on glass	E-beam heated C rod	[98]

7.5 × 10 ⁸ (C) To 9.6 × 10 ⁸ (T)	DLC on glass	Bias sputtered and plasma deposited	[99]
3. To 4 × 10 ⁹ (C)	DLC on quartz glass and Si	Ion source	[100]
0.5 To 3. × 10 ⁹ (C)	DlCon Si	Ion source	[101,102]
1.6 × 10 ⁹ (C)	DLC on glass	RF magnetron sputter	[103]
~ 10 ⁹ (C)	DlC on ZnS and ZnSe	Ion source	[104]
1.2 × 10 ⁹ (C)	DLC on Si	DC plasma reactor	[105]
9.4 To 139 × 10 ⁶ (T)	Diamond on Si	Microwave plasma	[106]
2.1 To 4.7 × 10 ⁹ (C)	Diamond on Si (100)	Filament	[107,108]

Angus [109] and Tsai and Bogy [110] have disclosed a quick survey on the issue of stress in DLC and diamond film coatings. As opposed to adhesion, the stress in films can be quantitatively measured. Generally, it can be performed by the beam deflection method, which was examined by Campbell [92]. Table 3 shows the investigations of quantitative measurements of the stress for films. Gille and Rau [100] analyzed the buckling of C-films on a glass substrate to infer internal stress. D. Nir [101,102,111] examined the stress for DLC deposition on Si and many sheets of steel prepared by a DC glow-discharge source. The stress did not seem to be identified with the H content of the film, which contradicted earlier assumptions made by Enke [97], Zelez [100], and Anttila [112]. In any case, the stress expanded at low temperatures at that point leveled at higher temperatures. Specht et al. [107,108] analyzed the strain effect on diamond films using X-ray diffraction.

In the view of understanding the methods of coating deposition by using sputtering deposition techniques [113], Ager et al. [114] discussed whether the shifting and broadening of the Raman line from film was due to stress. They observed that the diamond Raman line was moved by 2.5 cm⁻¹ to a higher frequency, which could be clarified by stress of 9.0 × 10⁸ Pa, which agreed with other measurements in Table 3. So far, in the view of bonding aspect, only adhesion strength has been considered, and it improved the mechanical properties of DLC films. This was resolved to a limited extent by the strength of the bonding between substrate and film [115–119].

The strength of this combination was based on their thermodynamic properties, as given in Table 4.

Table 4. Thermodynamic properties of carbides

Compound	$\Delta H^{\circ}f$ (25 °C) (kcal mol ⁻¹)	$\Delta G^{\circ}f$ (25 °C) (kcal mol ⁻¹)	Linear Coeff. of Thermal Expansion (at 25 °C) × 10 ⁻⁶ C ⁻¹	Reference
Al ₄ C ₃	-30.9	-29	----	[120]
CoC ₃	9.5	7.1	----	[120]
Cr ₃ C ₂	-21	-21.2	8.0	[120,121]
Cr ₃ C ₂	-9 to -29	-11 to -31	----	[122]
Fe ₃ C	5.0	3.5	----	[120]
MoC	34.4	----	5.95	[121]
Mo ₃ C ₂	-14	-14.1	----	[123]
Mo ₂ C	-11.5	-12.5	5.48	[121,123]
Mo ₂ C	----	----	7.8 to 9.3	[94]
Ni ₃ C	11.0	----	----	[120]
SiC	-16.5	-15.9	4.63	[121,123]
TaC	-34.6	-34.6	8.2	[121,123]
TaC	-32.3 to -53	-35 to -56	7.1	[94,122]
Ta ₂ C	-47	-47	----	[123]
TiC	-43.8	-43.8	6.52	[121,123]
TiC	-44.1	-45.8	8.0 to 8.6	[94,122]
UC	-21.1	----	9.47	[121,122]

UC ₂	21 to 30	----	6.32	[121,122]
U ₂ C ₃	-54	----	6.26	[120,121]
U ₂ C ₃	-49	----	----	[122]
WC	-9.09	-8.5	4.9	[120–122]
WC	-8.4	----	3.8 to 3.9	[94,123]
W ₂ C	-6.3 to -9.7	----	----	[122]

3.5. DLC Film Adhesion

The synthesis and property improvement process for DLC film has been implemented by Angus [109] and Tsai and Bogoy [110], who examined the bonding delamination phenomena. Angus et al. suggested that the best adhesion was obtained on substrates that formed carbides such as Si, Fe, and Ti. Table 5 lists four investigation reports and quantitative measurements of the adhesion strength. The last section in Table 5 gives a correlation to put the measured adhesion qualities in context.

Table 5. Adhesion strength of various films and their fabrication procedures.

Adhesion Strength (Pa)	Type of Film Process	Deposition	Measurement Technique	Reference
1 to 3×10^9 (0.1 to 0.3 J m^{-2})	DLC on glass	e-beam heated C rod	Film buckling analysis	[98]
4 to 7×10^{10} (4 to 7 J m^{-2})	DLC on glass	Electron and ion beam source	Film buckling analysis	[100]
$> 2. \text{ to } 2.8 \times 10^7$ (failure occurred in substrate)	DLC on ZnS (ZnSe with 200 to 1000 Å Ge or Si interlayer)	Iron source	Sebastation pull test	[124,125]
2×10^9	DLC on glass	RF magnetron sputtering	Scratch test	[103]

Several researchers have reported on adhesion of DLC films in a qualitative manner [97–105,111,112,124–135]. It may be difficult to compare the outcomes from these different papers, because of the stated conditions, substrates, and methods for examination approach of the coatings.

BN and SiC have been used to improve diamond bonding and nucleation on ZnS and Si [136]. Ti and Ta were used to improve the adhesion of the DLC on Si [135]. However, the bonding abilities need to improve as a part of the interlayers between substrate and DLC. Sometimes the interlayer materials are those components in carbide structures with free ions. It is only possible to vary the process input parameters by altering the techniques. For DLC films, these issues have not been considered in detail, but Murakawa and Watanabe [137] used a BN film on Si as an example.

The interlayer examination was fragmented, in any case, since it only considered the bonding of the interlayer to the C over layers. In iron, many compounds are extraordinary due to the significance of treated steels. This segment, consequently, considered the iron compound and alloys for increasing the C-films/substrates adhesion [138–142].

In several cases, thermodynamic qualities for iron alloys and compounds have been measured at elevated temperatures.

3.6 Recent Manufacturing Process

In the above subsections, we described the properties and characterizations of DLC coatings. However, little recent advancement of manufacturing characteristics was also noted. The significant major part of this discussion is focused on the latest investigation of spark and arc sources, high power impulse magnetron sputtering (HiPMS), structure and nonlinear optical properties, and texturing. Vacuum electro-spark alloying (VESA)

and pulsed cathode arc evaporation (PCAE) were investigated for the deposition of TiC-based coatings in inert (Ar) and reactive (C_2H_4) atmospheric conditions [143]. An investigation was done by using high-power impulse magnetron sputtering (HiPIMS) for the deposition of micrometer-thick DLC coatings over Si and steel substrates [144]. The adhesion on both sorts of substrates was ensured with an easy Ti interlayer, while the energy of contact ions was adjusted by using RF (radio frequency) biasing on the substrate at 100 V DC self-bias.

Recently published work revealed DLC films that contain 4–29% of Si and were deposited by reactive magnetron sputtering of C target [145]. H-free DLC films with embedded Cu nanoparticles, such as DLC: Cu, were increased by simultaneous DC magnetron sputtering with graphite and Cu points of view [146].

4. Applications of DLC Coatings

DLC coatings are used for several applications, which are highlighted for PVD coatings, generally apart from cutting tools, for high operational temperatures. DLC coatings are particularly helpful wherever a mixture of friction and wear reduction is required. DLC coats the forefronts of devices for the rapid, dry molding of troublesome uncovered surfaces of wood and Al, such as on vehicle dashboards. The better wear, erosion, and electrical properties of DLC make it an attractive material for clinical applications. Fortunately, DLC has been demonstrated to possess astounding bio-similarity. Typical applications include:

- Automotive: piston pins, rocker arms
- Medical: surgical tools, prosthetic applications
- Firearms: firearm slides, barrels, bolt carriers
- Industrial parts and machinery: pistons, plungers, gears, mechanical seals
- Injection molding: dies, ejector pins, slippery machine components
- Consumer products: wrist joint watches, jewelry, golf clubs

4.1. Carbon Coatings on Front Surface of Al Mirrors

In the current scenario, front surface mirrors created by single-point diamond machining of bulk Al were utilized for pivoting polygons, fluttering mirrors, and relay elements with optical force. This impact has been illustrated [147,148] in Al mirrors ensured with thin over coating of SiO_x , and is expected for use in the 8–12 μm spectral bands. This impact occurred for just one direction of polarization, RP, corresponding to the plane of occurrence. Comparable impacts were noticed for some other protective coatings and other metallic reflectors [149,150], making these coatings unsatisfactory for use in 8–12 μm thermal imaging systems on 45° mirrors.

The beginning of this impact has been distinguished, and has shown that it does not occur in DLC protective coatings [148]. An RSRE-coated polygon for a coaxial scanner is outlined in Figure 4.

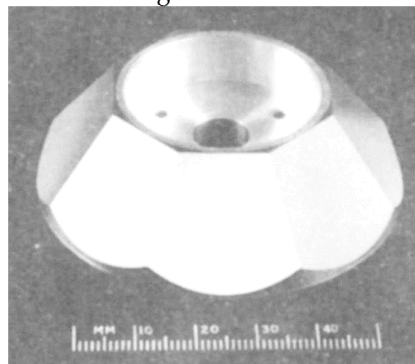


Figure 4. RSRE-coated polygon for a coaxial scanner [148].

4.2. DLC Coatings for Photothermal Conversion of Solar Energy

The primary objective of photo thermal solar energy transformation is to gather solar radiation to convert it into useful thermal conversion. There are two fundamental sorts of converter: the flat plate collector and the focusing collector. However, the heat losses are high from flat plate collectors, and their operating temperature is likely to be 70 °C. The focusing system has higher thermal efficiencies and working temperatures of approximately 100 °C are conceivable. It is common to eliminate thermal effects from both systems with circulating water [150–155].

4.3. Mechanical Applications of DLC Layers

In addition to the attractive properties of DLC, the material is additionally hard and artificially solid to make it helpful for securing metal objects from scratching and chemical reactions. This has been seen in various moving parts inside vehicle motors, and it has effectively reduced wear rates. The frictional properties of DLC were studied by Enke et al. [156], utilizing a ball-on-disc apparatus. They noticed an increase in the coefficient of friction from 0.01 to 0.19 μ with increasing humidity. A sharp increase in μ that occurred for relative humidities was around 1%. These results were in opposition to those for graphite and diamond reported by Bowden and Young [157], who noticed a reduction in μ with expanding water emission pressure. Kim et al. [158] studied the impacts of O on the frictions and wear of DLC films. Moreover, they considered the use of DLC films as protective overcoats on a thin-film magnetic recording disc. Comparative applications have been discussed by Tsui and Bogy [110] and by Marchon et al. [159], who related their perceptions with Raman and resistivity measurements. The utilization of DLC in magnetic and optical recoding discs would seem to offer promising market opportunities.

4.4. Electronic Device Applications of DLC

DLC films have been studied as both active and passive elements in devices. Their use in an exchanging-current thin-film electroluminescent device was reported by Kim et al. [160]. The emission that occurred during the breakdown of the DLC layer was wide-band, and seemed to be white. In another implement application, Kapoor et al. [161] explored the utilization of DLC films as the protector in metal–insulator–semiconductor (MIS) devices. The findings were not useful, owing to the low resistivity of the films and the enormous number of imperfections. Rothschild et al. [162] exhibited the utilization of DLC film as a method for high resolutions of semiconductor surfaces [163].

4.5. Medical Applications of DLC Layers

DLC films have received more attention within the last 20 years as candidate biomaterials due to their superior mechanical properties and biocompatibilities. In addition, C in several structures has been utilized for a number of biomedical applications. Tissue can adhere well to C implants and support a robust interface. Additionally, in the presence of blood, a protein layer is formed, which prevents the formation of blood clots at the C surface [164–167]. C fiber inserts can advance the fast ingrowth of tissue [168–175]. However, in recent years, several researchers have shown an interest in this application for the biomedical sector [176–180].

4.6. Others Applications of DLC

DLC coatings have found broad industrial applications, particularly in optical and electronic areas. They also have been effectively utilized in various tribological applications [181–183]. In tribological applications, DLC coatings were used successfully as coatings for ball bearings, where they decreased the friction coefficient between the ball and race; in shaving applications, where they increased the life of razor blades in wet shaving applications; and increasingly in automotive applications, such as racing engines and standard production vehicles. The structural and mechanical behaviors of DLC coatings

are the dependent factors of the deposition method and the incorporation of additional elements such as nitrogen, hydrogen, and silicon. These additional elements control the hardness of the resultant film, the level of residual stress, and the tribological properties. As DLC films increasingly become adopted for use in industry, knowledge of the factors that control their properties, and thus the ultimate performance of coated components in practical tribological applications, are becoming increasingly important.

Muthuraja et al. [184] developed a coating composition for improving the coating adhesion on high C steel, and progressively the coating morphology. Further, DLC coatings were employed by Grigoriew to enhance the strength of ceramic tools [185]. Recently, Podgornik et al. [186] demonstrated that a DLC/steel blend gave a smoother running in a measure when contrasted with DLC [187].

DLC coatings are an amorphous C material that exhibits typical diamond-like hardness and low-friction, characterized by the sp^3 -reinforced C and the structure. The proportion of sp^2 (graphically) and sp^3 (diamond-like) determines the properties of the DLC. The novel fabrication of DLC coatings that incorporated nanoparticles (WO_3/MoO_3) and PECVD for automobile applications has shown improvement within the adhesion properties of the DLC coatings [188].

DLC has been discovered to have great application in biomedical zones, where its biocompatibility and erosion obstruction permit it to be utilized in tribological applications.

5. Conclusions

DLC coatings have received more attention for various enhancements in distinct material properties since the last century. A viable approach for presenting and characterization of applications related to DLC coatings has been attempted. DLC coatings have quite alluring wear behavior that can be customized by modifying the C sp^2/sp^3 proportion.

Classifications of DLC coatings based on different considerations, while simultaneously providing their applications in a wide array of industrial sectors such as biomedical, marine, automobiles, and aerospace engineering, has been provided so that the reader understands the viability and importance of the DLC coating process. This work further highlights that much work needs to be done to develop DLC coatings by mixing composite material additives, which should be cost-effective.

The current literature shows that DLC coatings are one of the most promising coating processes for fulfilling the increasing demands where certain properties such as lower friction, good tribological behavior, and thermal characteristics are required. DLC coatings have importance in the hybrid industry, from clinical to automotive. Some of the fundamental difficulties with DLC coatings are in choosing the correct types of films for a particular application, and adhesion with other materials. More future investigation is expected to discover new/reformed DLC coatings with a combination of various influencing parameters and implementation of new methodologies.

Author Contributions: Conceptualization, D.K.R.; A.K.; A.B. and P.L.M.; methodology, D.K.R.; A.K. and P.L.M.; writing—original draft preparation, D.K.R.; A.K.; A.B. and P.L.M.; writing—review and editing, D.K.R. and P.L.M.; All authors have read and agreed to the published version of the manuscript.

Funding: This research received no external funding.

Institutional Review Board Statement: Not applicable.

Informed Consent Statement: Not applicable.

Data Availability Statement: Not applicable.

Conflicts of Interest: The authors declare no conflict of interest.

References

1. Robertson, J. Diamond-Like Amorphous, C. *Mater. Sci. Eng. R Rep.* **2002**, *37*, 129–281.
2. Kržan, B.; Novotny-Farkas, F.; Vizintin, J. Tribological behavior of tungsten-doped DLC coating under oil lubrication. *Tribol. Int.* **2009**, *42*, 229–235.
3. Evtukh, A.A.; Litovchenko, V.G.; Litvin, Y.M.; Fedin, D.V.; Dzyan, O.S.; Pedchenko, Y.N.; Chakhovskoi, A.G.; Felner, T.E. Silicon Doped Diamond-Like C Films as a Coating for Improvement of Electron Field Emission. Proceedings of the 14th International Vacuum Microelectronics Conference, Davis, CA, USA, 12–16 August, 2001, 295.
4. Louis, B. Amorphous Diamond, A New Super-Hard Form of C Created Under Ultrahigh Pressure; Science Daily: Rockville, MD, USA, 2011.
5. Treutler, C.P.O. *Surf. Coat. Technol.* **2005**, *200*, 1969–1975.
6. Van Der Kolk, G.J. In *Tribology of Diamond-Like C Films*, Springer Science + Business Media; C.; Donnet, C.; Erdemir, A.; Eds.; Llc. New York, NY, USA, 2008, 484–493.
7. Klaus, B.; Dieter, H. History of Diamond-Like C Films—From First Experiments to Worldwide Applications. *Surface Coat. Technol.* **2014**, *242*, 214–225.
8. Goglia, P.; Berkowitz, J.; Hoehn, J.; Xidis, A.; Diamond-like carbon applications in high density hard disc recording heads. Stover, L. *Diamond Relat. Mater.* **2001**, *10*, 271–277.
9. Ferrari, A. Diamond-like carbon for magnetic storage disks. *Surf. Coat. Technol.* **2004**, *180*, 180–181.
10. Schmellenmeier, H. Die Beeinflussung von festen Oberflächen durch eine ionisierte. *Exp. Tech. Phys.* **1953**, *1*, 49–68.
11. Schmellenmeier, H. Carbon layers with diamond structure. *Phys. Chem.* **1956**, *205*, 349–360.
12. König, H.; Helwig, G. Z. Thin Layers Formed from Hydrocarbons by Electron or Ion Bombardment. *Phys.* **1951**, *129*, 491–503.
13. Heisen, A. Über die Bildung dünner Kohleschichten in einer in Benzolatmosphäre brennenden Glimmentladung. *Ann. Phys.* **1958**, *457*, 23–35.
14. Heisen, A. *Optik* **1961**, *18*, 59–68.
15. Aisenberg, S.; Chabot, R. Ion-beam deposition of thin films of diamondlike carbon. *J. Appl. Phys.* **1971**, *42*, 2953–2958.
16. Aisenberg, S.; Chabot, R. Physics of ion plating and ion beam deposition. *J. Vac. Sci. Technol.* **1973**, *10*, 104–107.
17. Spencer, E.G.; Schmidt, P.H.; Joy, D.C.; Sansalone, F. Ion-beam-deposited polycrystalline diamondlike films. *J. Appl. Phys. Lett.* **1976**, *29*, 118–120.
18. Whitmell, D.S.; Williamson, R. The deposition of hard surface layers by hydrocarbon cracking in a glow discharge. *Thin Solid Films* **1976**, *35*, 255–261.
19. Holland, L. Some characteristics and uses of low-pressure plasmas in materials science. *J. Vac. Sci. Technol.* **1977**, *14*, 5–15.
20. Bewilogua, K.; Wagner, D. The effect of secondary electrons in the ion plating deposition of amorphous hydrogenated carbon (aC:H) films. *Vacuum* **1991**, *42*, 473–476.
21. Allen, S.M.; Thomas, E.L. *The Structure of Materials*; Wiley: New York, NY, USA, 1998, pp. 2.
22. Carbon Based Films-Classification and Designations ISO 20523:2017. *The International Organization for Standardization*; Vernier: Geneva, Switzerland, 2017.
23. Ohgoe, Y.; Hirakuri, K. K.; Saitoh, H.; Nakahigashi, T.; Ohtake, N.; Hirata, A.; Kanda, K.; Hiratsuka, M.; Fukui, Y. Classification of DLC films in terms of biological response. *Surf. Coat. Technol.* **2012**, *207*, 350–354.
24. Hiratsuka, M.; Nakamori, H.; Kogo, Y.; Sakurai, M.; Ohtake, N.; Saitoh, H. Correlation between Optical Properties and Hardness of Diamond-Like Carbon Films. *Solid Mech. Mater. Eng.* **2013**, *7*, 187–198.
25. Jacob, W.; Moller, W. On the structure of thin hydrocarbon films. *App. Phys. Lett.* **1993**, *63*, 1771–1773.
26. Fallon, P.J.; Veerasamy, V.S.; Davis, C.A.; Robertson, J.; Amaratunga, G.A.J.; Milne, W.I.; Koskinen, J. Properties of filtered-ion-beam-deposited diamondlike carbon as a function of ion energy. *Phys. Rev. B.* **1993**, *48*, 4777.
27. Polo, M. C.; Andujar, J.L.; Robertson, J.; Milne, W.I.; Preparation of tetrahedral amorphous carbon films by filtered cathodic vacuum arc deposition. *Diam. Relat. Mater.* **2000**, *9*, 663–667.
28. Lifshitz, Y.; Lempert, G.D.; Grossman, E.; Avigal, I.; Uzan-Saguy, C.; Kalish, R.; Kulik, J.; Marton, D.; Rabalais, J.W. Growth mechanisms of DLC films from C+ ions: Experimental studies. *Diam. Relat. Mater.* **1995**, *4*, 318–323.
29. Merkulov, V.I.; Lowndes, D.H.; Jellison, G.E.; Poretzky, A.A.; Geohegan, D.B. Field emission studies of smooth and nanostructured carbon films. *App. Phys. Lett.* **1999**, *73*, 1228.
30. P.; Koidl, C.; Wagner, B.; Dischler, J. Wagner And, M.; Ramsteiner, Plasma deposition, properties and structure of amorphous hydrogenated carbon films. *Mat. Sci. Forum.* **1990**, *52*, 41–70.
31. Zou, J.W.; Reichelt, K.; Schmidt, K.; Dischler, B. The deposition and study of hard carbon films. *J. App. Phys.* **1989**, *65*, 3914–3918.
32. Kessels, W.M.M.; Gielen, J.W.A.M.; van de Sanden, M.C.M.; van Ijzendoorn, L.J.; Schram, D.C. A model for the deposition of aC:H using an expanding thermal arc. *Surf. Coat. Technol.* **1998**, *98*, 1584–1589.
33. Schwarz-Selinger, T.; Von Keudell, A.; Jacob, W. Plasma chemical vapor deposition of hydrocarbon films: The influence of hydrocarbon source gas on the film properties. *J. App. Phys.* **1999**, *86*, 3968.
34. Tamor, M.A.; Vassell, W.C.; Carduner, K.R. Atomic constraint in hydrogenated "diamond-like" carbon. *App. Phys. Lett.* **1991**, *58*, 592–594.
35. Donnet, C.; Fontaine, J.; Lefebvre, F.; Grill, A.; Patel, V.; Jahnes, C. Solid state ¹³C and ¹H nuclear magnetic resonance investigations of hydrogenated amorphous carbon. *J. App. Phys.* **1999**, *85*, 3264–3270.

36. M.; Weiler, M.; Sattel, S.; Giessen, T.; Jung, K.; Ehrhardt, H.; Veerasamy, V.S.; Robertson, J. Preparation and properties of highly tetrahedral hydrogenated amorphous carbon. *Phys. Rev. B* **1996**, *53*, 1594.
37. Weiler, M.; Lang, K.; Li, E.; Robertson, J. Deposition of tetrahedral hydrogenated amorphous carbon using a novel electron cyclotron wave resonance reactor. *App. Phys. Lett.* **1998**, *72*, 1314–1316.
38. Gao, J.; Wang, Y.; Wu, H.; Liu, X.; Wang, L.; Yu, Q.; Li, A.; Wang, H.; Song, C.; Gao, Z.; et al. *Construction Of Sp³/Sp²C Interface In 3D N-Doped NanoC For The O Reduction Reaction; Angew. Chem. Int. Ed.* **2019**, *58*, 15089.
39. Wu, Z.; Zhang, X.; Xu, D.; Ge, J. Construction of Nitrogen-Doped C Nanosheets for Efficient and Stable O Reduction Electrocatalysis. *J. Electron. Mater.* **2021**, *50*, 1349–1357.
40. Jiangwei, C.; Longlong, H.; Chang, Y.; Yiwang, D.; Chun, Y.; Jieshan, Q.; Highly efficient & economic synthesis of CoS_{1.097}/nitrogen-doped C for enhanced triiodide reduction. *Carbon*, **2021**, *174*, 445–450.
41. Xia, Y.; Zhang, Z.; Qin, F.; Gao, J.; Wang, H.; Xu, Z.; Tan, X.; Liu, X.; Li, X.; Yin, Z. Electrocatalytic activity enhancement of N, P-doped C nanosheets derived from polymerizable ionic liquids. *J. Appl. Electrochem.* **2021**, *51*, 669–679.
42. Yu, X.; Lu, X.; Qin, G.; Li, H.; Li, Y.; Yang, L.; Song, Z.; An, Y.; Yan, Y. Large-scale synthesis of flexible TiO₂/N-doped C nanofibres. A highly efficient all-day-active photocatalyst with electron storage capacity; *Ceramics International*. **2020**, *46*, 12538–12547.
43. Yu, X.; Lai, S.; Xin, S.; Chen, S.; Zhang, X.; She, X.; Zhan, T.; Zhao, X.; Yang, D. Coupling of Iron Phthalocyanine at C Defect Site via π - π Stacking for Enhanced O Reduction Reaction. *Appl. Catal. B Environ.* **2020**, 119437.
44. Lu, Z.; Gao, D.; Yi, D.; Yang, Y.; Wang, X.; Yao, J. sp²/sp³ Hybridized Carbon as an Anode with Extra Li-Ion Storage Capacity. Construction and Origin. *ACS Central Sci.* **2020**, *6*, 1451–1459, doi:10.1021/acscentsci.0c00593.
45. Wang, Y.; Suo, B.; Shi, Y.; Yuan, H.; Zhu, C.; Chen, Y. General Fabrication of 3D Hierarchically Structured Bamboo-like Nitrogen-Doped C Nanotube Arrays on 1D Nitrogen-Doped C Skeletons for Highly Efficient Electromagnetic Wave Energy Attenuation; *ACS Applied Mat. Interfaces*. **2020**, *12*, 40691–40701.
46. Muguruma, T.; Iijima, M.; Kawaguchi, M.; Mizoguchi, I. Effects of sp²/sp³ Ratio and Hydrogen Content on In Vitro Bending and Frictional Performance of DLC-Coated Orthodontic Stainless Steels. *Coatings* **2018**, *8*, 199.
47. Yimin, Lu, Guojun, Huang, Sai Wang, Chaowei Mi, Shangfang Wei, Fangtao Tian, Wei Li, Haiyuan Cao, Yong Cheng, A Review on Diamond-like C Films Grown by Pulsed Laser Deposition. *Appl. Surf. Sci.* **5 November 2020**, 148573.
48. Zhong, W.X.; Zhao, X.R.; Qin, J.Y.; Yang, J. An Active Hybrid Electrocatalyst with Synergized Pyridinic Nitrogen-Cobalt and O Vacancies for Bifunctional O Reduction and Evolution. *Chin. J. Chem.* **2021**, *39*, 655–660.
49. Lemoine, P.; Quinn, J.P.; Maguire, P.D.; McLaughlin, J.A.D.; Measuring the thickness of ultra-thin diamond-like carbon films. *Carbon* **2006**, *44*, 2617.
50. Sarakinos, K.; Braun, A.; Zilkens, C.; Mrazek, S.; Schneider, J.M.; Zoubos, H.; P. Patsalas. Exploring the potential of high power impulse magnetron sputtering for growth of diamond-like carbon films. *Surf. Coatings Technol.* **2012**, *206*, 2706–2710.
51. Chhowalla, M.; Robertson, J.; Chen, C.W.; Silva, S.R.P.; J.; A.G.A. Amaratunga. Influence of ion energy and substrate temperature on the optical and electronic properties of tetrahedral amorphous carbon (ta-C) films. *J. Appl. Phys.* **1997**, *81*, 139–145.
52. Kamata, K.; Inoue, T.; Sugai, K.; Saitoh, H.; Maruyama. *J. Appl. Phys.* **1995**, *78*, 1394.
53. Ferrari, A.C.; Kleinsorge, B.; Adamopoulos, G.; Robertson, J.; Milne, W.I.; Stolojan, V.; Brown, L.M.; Libassi, A.K.A.B. Tanner. *J. Non-Cryst. Solids*. **2000**, *266*, 266–269.
54. Libassi, A. C.; Ferrari, V.; Stolojan, B. K.; Tanner, J.; Robertson, J.; M. Brown. *Diamond Relat. Mater.* **2000**, *9*, 771.
55. Tan, M.; Zhu, J.; Liu, A.; Jia, Z.; Han, J. Effects of mass density on the micro hardness and modulus of tetrahedral amorphous carbon films. *Mater. Lett.* **2007**, *61*, 4647.
56. Chua, H.C.; Teo, K.B.K.; Tsai, T.H.; Milne, W.I.; Sheeja, D.; Tay, B.K.D. Correlation of surface, mechanical and microproperties of tetrahedral amorphous carbon films deposited under different magnetic confinement conditions. *Schneider. Appl. Surf. Sci.* **2004**, *221*, 455.
57. Pastorelli, R.; Ferrari, A.C.; Beghi, M.G.; Bottani, C.E.; Robertson, J. Elastic constants of ultrathin diamond-like carbon films. *Diamond Relat. Mater.* **2000**, *9*, 825.
58. Paik, N. High density DLC films prepared using a magnetron sputter type negative ion source. *Diamond Relat. Mater.* **2005**, *14*, 196.
59. Aijaz, A.; Sarakinos, K.; Lundin, D.; Brenning, N.; Helmersson, U. A strategy for increased carbon ionization in magnetron sputtering discharges. *Diamond Relat. Mater.* **2012**, *23*, 1.
60. Logothetidis, S.; Patsalas, P.; Gioti, M.; Galdikas, A.; Pranevicius, L. Growth kinetics of sputtered amorphous carbon thin films composition studies and phenomenological model. *Thin Solid Films* **2000**, *376*, 56.
61. Ferrari, A.C.; Libassi, A.; Tanner, B.K.; Stolojan, V.; Yuan, J.; Brown, L.M.; Rodil, S.E.; Robertson, B.K.A.J. Density SP³ fraction, and cross sectional structure of amorphous carbon films determined by X-ray reflectivity and electron energy-loss spectroscopy. *Phys. Rev. B* **2000**, *62*, 11089.
62. Ferrari, C.; Robertson, J. Interpretation of Raman spectra of disordered and amorphous carbon. *Phys. Rev. B* **2000**, *61*, 14095.
63. Casiraghi, A.; Ferrari, C.; Robertson, J. Raman spectroscopy of hydrogenated amorphous carbon. *Phys. Rev. B* **2005**, *72*, 085401.
64. Donnet, J.R.C.; Erdemir, A.; Eds.; *Tribology of Diamond-Like C Films. Fundamentals and Applications*; Springer: Berlin/Heidelberg, Germany, 2008, 13–24.
65. Tian, J.; Zhang, Q.; Zhou, Q.; Yoon, S.F.; Ahn, J.; Wang, S.G.; Li, J.Q.; Yang, A.D. Study of well adherent DLC films deposited on piezoelectric LiTO₃ substrate. *Appl. Surf. Sci.* **2005**, *239*, 255.

66. Robertson, D.J. Deposition mechanisms for promoting SP³ bonding in diamond-like carbon. *Relat. Mater.* **1993**, *3*, 361.
67. Hatada, R.; Flege, S.; Ashraf, M.N.; Timmermann, A.; Schmid, C.; Ensinger, W. The Influence of Preparation Conditions on the Structural Properties and Hardness of Diamond-Like C Films, Prepared by Plasma Source Ion Implantation. *Coatings* **2020**, *10*, 360.
68. Ito, H.; Yamamoto, K. Mechanical and tribological properties of DLC films for sliding parts. *Kobelco Technol. Rev.* **2017**, *35*, 55–60. Available online: https://www.kobelco.co.jp/english/ktr/ktr_35.html (accessed on 1 December 2020).
69. Písařík, P.; Jelínek, M.; Kocourek, T.; Remsa, J.; Zemek, J.; Lukeš, J.; Šepitka, J. Influence of diamond and graphite bonds on mechanical properties of DLC thin films. *J. Phys. Conf. Ser.* **2015**, *594*, 012008.
70. Johnson, J.A.; Woodford, J.B.; Chen, X.; Andersson, J.; Erdemir, A.; Fenske, G.R. Insights into ‘near frictionless carbon films’. *Appl. Phys.* **2004**, *95*, 7765.
71. Sanchez-Lopez, J.C.; Erdemir, A.; C.; C.D.; Rojas, A.T. Friction-induced structural transformations of diamond like carbon coatings under various atmospheres. *Surf. Coat. Technol.* **2003**, *163*, 444.
72. Aurang, P.; Demircioglu, O.; Es, F.; Turan, R.; Unalan, H.E. ZnO Nanorods as Antireflective Coatings for Industrial-Scale Single-Crystalline Silicon Solar Cells. *J. Am. Ceram. Soc.* **2013**, *96*, 1253–1257.
73. Gao, G.T.; Mikulski, P.T.; Harrison, J.A. Molecular scale tribology of amorphous carbon coatings: Effects of film thickness, adhesion and long range interaction. *J. Am. Chem. Soc.* **2002**, *124*, 7202.
74. Gao, G.T.; Mikulski, P.T.; Chateauneuf, G.M.; Harrison, J.A. The effects of film structure and surface hydrogen on the properties of amorphous carbon films. *J. Phys. Chem. B.* **2003**, *107*, 11082.
75. Bilek, M.M.M.; Mckenzie, D.R.; Moeller, W. Use of low energy and high frequency PBII during thin film deposition to achieve relief of intrinsic stress and microstructural changes. *Surf. Coat. Technol.* **2004**, *186*, 21.
76. Bilek MM, Verdon M, Ryves L, Oates TW, Ha CT, McKenzie DR. A model for stress generation and stress relief mechanisms applied to as deposited filtered cathodic vacuum arc amorphous carbon films. *Thin Solid Films* **2005**, *482*, 69.
77. Memming, R.; Tolle, H.J.; Wierenga, P.E. Properties of polymeric layers of hydrogenated amorphous carbon produced by a plasma-activated chemical vapor deposition process II: Tribological and mechanical properties. *Thin Solid Films* **1986**, *143*, 31.
78. Klages, P.; Memming, R. Microstructure and physical properties of metal-containing hydrogenated carbon films. *Mater. Sci. Forum.* **1990**, *52*, 609.
79. Available online: <Http://Www.Ist.Fraunhofer.De/English/C-Products/Tab/Complete.Html>. (accessed on 1 December 2020).
80. Muhl, S.; Mendez, J.; A review of preparation of carbon nitride films. *Diam, M. Relat. Mater.* **1999**, *8*, 1809–1830.
81. K. Oguri and T.; Arai, Tribological properties and characterization of diamond-like carbon coatings with silicon prepared by plasma-assisted chemical vapour deposition. *Surf. Coat. Technol.* **1991**, *47*, 710.
82. Zhang, S.; Bui, X. L.; Zeng, X.L.; Li, X.M. Towards high adherent and tough aC coatings. *Thin Solid Films* **2005**, *482*, 138.
83. Kaczorowski, W.; Świątek, H.; Łuczak, K.; Głuszek, M.; Cłapa, M. Impact of Plasma Pre-Treatment on the Tribological Properties of DLC Coatings on PDMS Substrates. *Materials* **2021**, *14*, 433.
84. Wang Y, Wang Y, Kang J, Ma G, Zhu L, Wang H, Fu Z, Huang, H.; Yue, W. Tribological Properties of Ti-Doped Diamond Like C Coatings Under Boundary Lubrication with ZDDP, *J. Tribol. ASME.* **2021**, *143*, 091901.
85. Fiaschi, G.; Rota, A.; Ballestrazzi, A.; Marchetti, D.; Vezzalini, E.; Sergio, V.A.; Chemical, Mechanical, and Tribological Analysis of DLC Coatings Deposited by Magnetron Sputtering. *Lubricant* **2019**, *7*, 38.
86. Field, J.E. *The Properties of Diamond*, Academic Press Inc.: New York, NY, USA, 1979, pages. 678. (ISBN 10-0122553500, ISBN 13: 978-0122553500).
87. Outka, A.; Hsu, W.L.; Boehme, D.R.; Yang, N.Y.C.; Ottesen, D.K.; Johnsen, H.A.; Headley, T.J.; Clift, W.M. Sandia Report Sand94-8219, Uc-404, Unlimited Release Printed February, 1994.
88. Hoffman, R.W. The Mechanical Properties of Thin Condensed Films. In *Physics of Thin Films*; Hass, G.; Thun, R.E.; Eds.; Academic: New York, NY, USA, 1966, p. 266.
89. Chopra, K.L. *Thin Film Phenomena*; Mcgraw-Hill: New York, NY, USA, 1969.
90. Field, J.E. Strength and Fracture Properties of Diamond. In *The Properties of Diamond*; Field, J.E.; Ed.; Academic, New York, NY, USA, 1979, p. 281.
91. Gray, E.; Ed. *American Institute of Physics Handbook*. 3rd Edition Ed.; Mcgraw-Hill, New York, NY, USA, 1972.
92. Campbell, S. Mechanical Properties of Thin Films. In *Handbook of Thin Films Technology*, Maissel, L.I.; Glang, R.; Eds.; Mcgraw-Hill: New York, NY, USA, 1970, p. 12.
93. Weast, R.C.; Ed. *Handbook of Chemistry and Physics*, 70th Ed.; Crc Press, Boca Raton, FL, USA, 1989.
94. Holleck, H. Material selection for hard coatings. *J. Vac. Sci. Technol. A* **1986**, *4*, 42661.
95. Gere, J.M.; Timoshenko, S.P. *Mechanics of Materials*, 3rd Ed.; Pws-Kent, Boston, USA, 1990.
96. Jaccodine, R.J.; Schlegel, W.A. Measurement of strains at SiO₂ interface. *J. Appl. Phys.*, **1966**, *37*, 2429.
97. Enke, K. Some new results on the fabrication of and the mechanical, electrical and optical properties of i-carbons layers. *Thin Solid Films* **1981**, *8*, 80227.
98. Matuda, N.; Baba, S.; Kinbara, A. Internal stress, young's modulus and adhesion energy of carbon films on glass substrate. *Thin Solid Films* **1981**, *8*, 1301.
99. Zelez, J. Low stress carbon like carbon films. *J. Vac. Sci. Technol. A* **1983**, *1*, 305.
100. Gille, B.R. Buckling instability and adhesion of carbon layers. *Thin Solids Films* **1984**, *120*, 109.

101. Outka DA, Hsu WL, Phillips K, Boehme DR, Yang NY, Ottesen DK, Johnsen HA, Clift WM, Headley TJ. Compilation of diamond like carbon properties for barriers and hard coatings, *ostiv*, 1994., 10151476.
102. Nir. Intrinsic stress in diamond-like carbon films and its dependence on deposition parameters. *Thin Solid Films* **1987**, *146*, 27.
103. Kikuchi, A.; Baba, S.; Kinbara, A. Measurement of the adhesion of silver films to glass substrate. *Thin Solid Films* **1985**, *343–349*.
104. First International Symposium on Diamond and Diamond like Films. Proceedings, *Electrochemical. Society*; BK & Insrt edition, June 1, 1989, 12–89. ISBN-10: 9990172730, ISBN-30: 978–9990172737.
105. Ham, M.; Lou, K.A. Diamond like carbon films grown by a large scale direct current plasma-chemical vapor deposition reactor: System design ,film characteristics and applications. *J. Vac. Sci. Technol. A* **1990**, *8*, 2143.
106. Berry BS, Pritchett WC, Cuomo JJ, Guarnieri CR, Whitehair SJ. Internal stress and elasticity of synthetic diamond films. *Appl. Phys. Lett.* **1990**, *57*, 302.
107. Specht, E.D.; Clausing, R.E.; Heatherly, L. Measurement of crystalline strain and orientation in diamond films grown by chemical vapor deposition. *J. Mater. Res.* **1990**, *5*, 2351.
108. Clausing RE, Heatherly L, Specht ED, More KL, Begun GM. Growth mechanism, film morphology, texture and stresses for three types of HFCVD diamond film growth. *Carbon*, **1990**, *28*, 762.
109. Angus, J.C.; Koidl, P.; Domitz, A.S. C Thin Films. In *Plasma Deposited Thin Films*; Mort, J.; Jansen, F.; Eds.; Crc Press, Ln, C.; Boca Raton, FL, USA, 1986, p. 89.
110. Tsai, H.-C.; Bogy, D.B. J.Charecterization of diamond like carbon films and their applications as overcoats on thin film media for magnetic recording. *Vac. Sci. Technol. A* **1987**, *5*, 3287.
111. Nir. Stress relief forms diamond-like carbon thin films under internal compressive stress. *Thin Solid Films* **1984**, *112–141*.
112. Anttila A, Koskinen J, Lappalainen R, Hirvonen JP, Stone, D.; Paszkiet, C. Comparison of diamond like coatings with C+ and various hydrocarbon ion beams. *Appl. Phys. Lett.* **1987**, *50*, 132.
113. Shrnivashan, N.; Bhaskar, L.K.; Kumar, R.; Bhargeti, S. Residual Stress Gradient and Relaxation Upon Fatigue Deformation of Diamond-Like C Coated Aluminum Alloy in Air and Methanol Environments. *Mat. Design* **2018**, *160*, 303–312.
114. Ager, J.W.; Veirs, D.K.; Rosenblatt, G.M. Spatially resolved Raman studies of diamond films grown by chemical vapor deposition. *Phys. Rev. B.* **1991**, *6491*.
115. Stoney, G.G. The tension of metallic films deposited by electrolysis. *Proc. Roy. Soc.* **1909**, *32*, 172.
116. Spear, K.E Diamond ceramic coatings of the future. *J. Am. Ceram. Soc.* **1989**, *72*, 171.
117. Hull, T.; Colligon, J.S.; Measurement of thin film adhesion. Hill, A.A.E. *Vacuum* **1987**, *37*, 327.
118. Zhang, B.; Zhou, L. Effect of sandblasting on adhesion strength of diamond coatings. *Thin Solid Films*, **1997**, *307*, 21–28.
119. Halpern, J Determination and significance of transition metal-alkyl bond dissociation energy.. *Acc. Chem. Res.* **1982**, *15*, *8*, 238–244.
120. Rossini, F.D. Selected Values of Chemical Thermodynamic Properties, National Bureau of Standards Circular 500; US Government Printing Office: Washington, DC, USA, 1952.
121. Shaffer, P.T.B. Plenum Press Handbooks of High-Temperature Materials; Plenum: New York, NY, USA, 1964.
122. Storms, K. Tile Refractory Carbides; Academic, New York, NY, USA, 1967.
123. Schick, H.L. Thermodynamics of certain refractory compounds. Academic press **1966**, *2*.
124. Mirtich MJ, Nir, D.; Swec, D.; Banks, B. The use of intermediate layers to improve the adherence of diamond like carbon films on Zns and ZnSe. *J. Vac. Sci. Technol. A* **1986**, *4*, 2680.
125. Swec DM, Mirtich MJ, Nir, D.; Banks BA. Comparison of protective coatings for infrared transmitting windows. *J. Vac. Sci. Technol. A* **1986**, *4*, 3030.
126. Anton, P.GM.B.H. Characterization of Hard Coatings–Part, I. DLC Coatings. AZoM. 14 February 2020, Retrieved on 11 March 11, 2021.sponshered by Anton Paar GmbH.
127. Miyoshi, K.; Buckley, D.H. Adhesion and friction of single crystal diamond in contact with transition metal. *Appl. Surf. Sci.* **1980**, *6161*.
128. Shibuki K, Yagi M, Saijo K, Takatsu, S. Adhesion strength of diamond films on cemented carbide substrates. *Surf. Coat. Technol.* **1988**, *3*, 295.
129. Saijo K, Yagi M, Shibuki K, Takatsu, S. The improvement of the adhesion strength of diamond films. *Surf. Coat. Technol.* **1990**, *43*, 30.
130. Grill, A.; Meyerson, B.; Patel, A.V Interface modifications for improving the adhesion of aC: H films to metals. *J. Mater. Res.* **1988**, *3*, 214.
131. Mccune, R.C. Stresses and Mechanical Properties. *Mater. Res. Soc.* **1989**, *50*, 261.
132. Murakawa, M.; Takeuchi, S. Quantitative adhesion strength measurement of diamond coatings. *Thin Solid Films* **1989**, *443–450*.
133. Kuo, C.-T.; Yen, T.-Y.; Huang, A.T.-H. Adhesion and tribological properties of diamond films on various substrates. *J. Mater. Res.* **1990**, *5*, 2515–2523.
134. Galuska, A.A Copper glassy carbon adhesion: Improvement through 27 Al+ implantation. *Surf. Coat. Technol.* **1990**, *975–985*.
135. Wang, M.; Jiang, X.; Stritzker, A.B. Adhesion of hydrogenated amorphous carbon films on silicon substrates and its enhancement. *Thin Solid Films* **1991**, *97*, 57–66.
136. Hartnett T, Miller R, Montanari D, Willingham C, Tustison, R. Intermediate layers for the deposition of polycrystalline diamonds films. *J. Vac. Sci. Technol. A.* **1990**, *8*, 2129.

137. Murakawa, M.; Watanabe, S.; Tribological properties of cubics amorphous and hexagonal boron nitride films. *Surf. Coat. Technol.* **1990**, *145*.
138. Abermann, R.; Kramer, R.; Mäser, J. Structure and internal stress in ultra-thin silver films deposited on MgF₂ and SiO substrate. *Thin Solid Films* **1978**, *52*, 215–229.
139. Thurner, G.; Abennaram, R. Internal stress and structure of ultra-high vacuum evaporated chromium and iron films and their dependence on substrate temperature and oxygen particle pressure during deposition. *Thin Solid Films* **1990**, *192*, 277–285.
140. Staudhammer, K.P.; Mutt, L.E. Atlas T₂ Binary Alloys; Marcel Dekker Inc: New York, NY, USA, 1973.
141. NBS. Selected Values of the Thermodynamic Properties of Binary Alloys; American Society for Metals: Metals Park, OH, USA, 1973.
142. Metals Reference Book, 5th ed. Ed.; C.J.S.; Ed.; Butterworths, Boston, MA, USA, 1976.
143. Kiryukhantsev-Korneev P, Sytchenko A, Sheveyko A, Moskovskikh D, Vorotylo, S. Two-Layer Nano composite TiC-Based Coatings Produced by a Combination of Pulsed Cathodic Arc Evaporation and Vacuum Electro-Spark Alloying. *Materials* **2020**, *13*, 547.
144. Vitelaru C, Parau AC, Constantin LR, Kiss AE, Vladescu A, Sobetkii A, Kubart, T. A Strategy for Alleviating Micro Arcing During HiPMS Deposition of DLC Coatings. *Materials* **2020**, *13*, 1038.
145. Meškiniš Š, Vasiliauskas A, Andrulevičius M, Peckus D, Tamulevičius, S.; Viskontas, K. Diamond Like C Films Containing Si. Structure and Non-linear Optical Properties. *Materials* **2020**, *13*, 1003.
146. Meškiniš Š, Vasiliauskas A, Viskontas K, Andrulevičius M, Guobienė, A.; Tamulevičius, S. Hydrogen-Free Diamond Like C Films with Embedded Cu- Nanoparticles. Structure, Composition and Reverse Saturable Absorption Effect. *Materials* **2020**, *13*, 760.
147. Cox, J.T.; Hass, G.; Hunter, W.R. Infrared Reflectance of Silicon Oxide and Magnesium Fluoride Protected Aluminium Mirrors at Various Angles of Incidence From 8 μm to 12 μm. *Appl. Opt.* **1975**, *14*, 1247.
148. Lettington, A.H.; Ball, G.J. The Protection of Front Surfaced Aluminium Mirrors with Diamond-Like C Coatings for Use in the Infrared. Rsrre Memorandum No. 3295, 1981.
149. Pellicori, S.F. Infrared Reflectance of a Variety of Mirrors at 480 Incidences. *Appl. Opt.* **1978**, *17*, 3335.
150. Cox, J.T.; Hass, G. Aluminium Mirrors Al₂O₃ Protected with High Reflectance at Normal but Greatly Decreased Reflectance at Higher Angles of Incidence in the 8–12 μm Region. *Appl. Opt.* **1978**, *17*, 333.
151. Hahn, R.E.; Seraphin, B.O. Spectrally Selective Surfaces for Photo Thermal Energy Conversion. *Phys. Thin Films* **1978**, *10*, 1.
152. Drummeter, L.F.; Hass, G. *Phys. Thin Films* **1964**, *2*, 305.
153. Seraphin, B.O. Chemical Vapour Deposition of Spectrally Selective Surfaces. *J. of Vacuum Science and Technology*, **1979**, *16*, 193–196.
154. Janai, M. A.; Allred, D. D.; Booth, D. C. & Seraphin, B.O. Optical Properties and Structure of Amorphous Silicon Films Prepared by Cvd. *Solar Energy Mater.* **1979**, *1*, 11.
155. Ball, G.J.; Lettington, A.H. Diamond-Like C Coatings for The Photo Thermal Conversion of Solar Energy. Rsrre Memorandum No. 3617, 1983.
156. Enke, K.; Dimigen, H.; Hubsch, H. Frictional Properties of Diamond-Like C Layers. *Appl. Phys. Lett.* **1980**, *36*, 291.
157. Bowden, F.P.; Young, J.E. Friction of Diamond, Graphite, and C and the Influence of Surface Films. *Proc. R. Soc. Lond. A* **1951**, *208*, 444.
158. Kim, D.S.; Fischer, T.E.; Gallois, B. The Effects of Oand Humidity on Friction and Wear of Diamond-Like C Films. *Surf. Coat. Technol.* **1991**, *49*, 537.
159. Marchon, B.; Heiman, N.; Khan, M.R.; Lautie, A.; Ager, J.W.; Veirs, D.K. Raman And Resistivity Investigations of C Overcoats of Thin-Film Media. Correlations with Tibological Properties. *J. Appl. Phys.* **1991**, *69*, 5748.
160. Kim, S. B.; Wager, J.F. Diamond-Like C Films for Electroluminescent Applications. *Surf. Coat. Technol.* **1990**, *43*, 99.
161. Kapoor, V.J.; Mirtich, M.J.; Banks, B.A. Diamond-Like C Films on Semiconductors for Insulated-Gate Technology. *J. Vac. Sci. Technol.* **1986**, *A4*, 1013.
162. Rothschild, M.; Arnone, C.; Ehrich, D.J. Eximer-Laser Etching of Diamond and Hard C Films by Direct Writing and Optical Projection. *J. Vac. Sci. Technol.* **1986**, *B4*, 310.
163. Marotta, E.; Bakhru, N.; Grill, A.; Patel, V.; Meyerson, B. Diamond-Like C as an Electrical Insulator of Copper Devices for Chip Cooling. *Thin Solid Films* **1991**, *206*, 188–191.
164. Jenkins, G.M. Biomedical Applications of Cs and Graphites. *Clin. Phys. Physiol. Meas.* **1980**, *1*, 171–194.
165. Jenkins, G.M.; De Carvallo, F.X. Biomedical Applications of carbon Fibre Reinforced Cin Implanted Prostheses. *Carbon.* **1977**, *15*, 33–37.
166. Thomson, L.A.; Law, F.C.; Rushton, N.; Franks, J. Biocompatibility of Diamond-Like, C. *Coat. Biomater.* **1991**, *12*, 37.
167. Feng Wen, Jiaqi Liu, Jianlu Xue, The Studies of Diamond-Like C Films as Biomaterials. Review. *Colloid Surf. Sci.* **2017**, *2*, 81–95.
168. Narin, S.; Shuichi, W.; Nutthanun, M. Elements-Added Diamond-Like C Film for Biomedical Applications. *Adv. Mater. Sci. Eng. Hindawi* **2019**, *2019*, 6812092.
169. Zhou H, Jiang M, Xin Y, Sun G, Long S, Bao S, Cao, X.; Ji, S.; Jin, P. Surface Deposition of Graphene Layer for Bioactivity Improvement of Biomedical 316 Stainless Steel. *Mater. Lett.* **2017**, *192*, 123–127.
170. Amanov, A.; Lee, S.W.; Pyun, Y.S. Low Friction and High Strength of 316L Stainless Steel Tubing for Biomedical Applications. *Mater. Sci. Eng. C* **2017**, *71*, 176–185.

171. Bociaga, D.; Kaminska, M.; Sobczyk-Guzenda, A.; Jastrzebski, K.; Swiatek, L.; Olejnik, A. Surface Properties and Biological Behaviour of Si-DLC Coatings Fabricated by A Multi-Target DC-RF Magnetron Sputtering Method for Medical Applications. *Diam. Relat. Mater.* **2016**, *67*, 41–50.
172. Moolsradoo, N.; Watanabe, S. Influence of Elements on The Corrosion Resistance of DLC Films. *Adv. Mater. Sci. Eng.* **2017**, *3571454*, 6.
173. Ray, S.C.; Pong, W.F.; Papakonstantinou, Iron, Nitrogen and Silicon Doped Diamond Like C (DLC) Thin Films. A Comparative Study. *Thin Solid Films.* **2016**, *610*, 42–47.
174. Wang, J.; Ma, J.; Huang, W.; Wang, L.; He, H.; Liu, C. The Investigation of The Structures and Tribological Properties Of F-DLC Coatings Deposited on Ti-6Al-4V Alloys. *Surf. Coat. Technol.* **2017**, *316*, 22–29.
175. Yu H, Liu Y, Wang Y, Liu, L.; Li, B.; Li, Y.; Zhao, X. A Study on Poly (N-Vinyl-2-Pyrrolidone) Covalently Bonded Niti Surface For Inhibiting Protein Adsorption. *Progress in Natural Science. Mater. Int.* **2016**, *26*, 584–589.
176. Kumar, A.M.; Suresh, B.; Das, S.; Obot, I.B.; Adesina, A.Y.; Ramakrishna, S. Promising Bio-Composites of Polypyrrole And Chitosan. Surface Protective and in Vitro Biocompatibility Performance on 316L SS Implants. *Carbohydr. Polym.* **2017**, *173*, 121–130.
177. PremKumar, K.P.; Duraipandy, N.; Syamala, K.N.; Rajendran, N. Antibacterial Effects, Biocompatibility and Electrochemical Behavior of Zinc Incorporated Niobium Oxide Coating On 316L SS For Biomedical Applications. *Appl. Surf. Sci.* **2018**, *427*, 1166–1181.
178. Wachesk, C.C.; Trava-Airoldi, V.J.; Da-Silva, N.S.; Lobo, A.O.; Marciano, F.R. The Influence of Titanium Dioxide on Diamond-Like C Biocompatibility for Dental Applications. *J. Nanomater.* **2016**, *8194516*, 7.
179. Gotzmann, G.; Beckmann, J.; Wetzel, C.; Scholz, B.; Herrmann, U.; Neunzehn, J. Electron-Beam Modification of DLC Coatings for Biomedical Applications. *Surf. Coat. Technol.* **2017**, *311*, 248–256.
180. Bociaga D, Sobczyk-Guzenda A, Szymanski W, Jedrzejczak A, Jastrzebska A, Olejnik A, Jastrzebski, K. Mechanical Properties, Chemical Analysis and Evaluation of Antimicrobial Response of Si-DLC Coatings Fabricated on AISI 316 LVM Substrate by A Multi-Target DC-RF Magnetron Sputtering Method for Potential Biomedical Applications. *Appl. Surf. Sci.* **2017**, *417*, 23–33.
181. Schäfer, L.; Gäbler, J.; Mulcahy, S.; Brand, J.; Hieke, A.; Wittorf, R. Tribological Applications of Amorphous C and Crystalline Diamond Coatings. Proc. 43rd Svc Ann. Techn. Conf., Denver, KL, USA, April 2000, Society of Vacuum Coaters.
182. M. Ga Hlin, M. Larsson and P. Hedenqvist. 'Me-C. H Coatings in Motor Vehicles', *Wear*, **2001**, *249*, 302–209.
183. Brand, J.; Beckmann, C.; Filfil, T.M.A.T. Reduzierung Von Reibungsverlusten Im Ventiltrieb Durch Beschichtungen, Vdi Report, Vdi, Du Sseldorf, Germany, **1999**, *1472*, 299–312.
184. Muthuraja, A.; Naik, S.; Rajak, D.K.; Pruncu, C.I.; Experimental investigation on chromium-diamond like carbon (Cr-DLC) coating through plasma enhanced chemical vapour deposition (PECVD) on the nozzle needle surface. *Diam. Relat. Mater.* **2019**, *100*, 107588.
185. Grigoriev, S.; Volosova, M.; Fyodorov, S.; Lyakhovetskiy, M.; Seleznev, A.; DLC-coating Application to Improve the Durability of Ceramic Tools. *J. Mater. Eng. Perform.* **2019**, *28*, 4415–4426.
186. Podgornik, S.J.; Hogmark, S. Dlc Coating of Boundary Lubricated Components. Advantages of Coating One of the Contact Surfaces Rather Than Both or None. *Tribol. Int.* **2003**, *36*, 843–849.
187. Persson, K.; Gahlin, R. Tribological Performance of a Dlc Coating in Combination with Water-Based Lubricants. *Tribol. Int.* **2003**, *36*, 851–855.
188. Kolawole, F.O.; Kolawole, S.K.; Varela, L.B.; Owa, A.F.; Ramirez, M.A.; Tschiptschin, A.P.; Diamond-Like C (DLC) Coatings for Automobile Applications. In: *Engineering Applications of Diamond*. IntechOpen: London, USA. 2020.